

Figure 5. Energy level diagram of the $[\text{NbO}_2\text{F}_3]^{2-}$ ion. The arrow indicates the highest occupied molecular orbital, coefficients for which are given in the text.

the O_2^- ion and the fact that one of the principal values of the g tensor lies along the $\text{O}_1\text{-O}_2$ bond direction.

Conclusions

The present work on the DPPN X-ray structure has removed the existing ambiguity about its previously reported space group

and confirmed it to be $C2$. The stability and observability of the $[\text{NbO}_2\text{F}_3]^-$ species at room temperature are quite interesting, while most of the Nb species like the $[\text{NbOF}_3]^-$ hole species are observable only below 195 K. A reduction in symmetry from O_h to C_{2v} , which resulted in the unpaired electron occupying a non-degenerate nonbonding MO, is probably the reason that the radical could give an observable spectrum at room temperature. In other words, the "hole" is almost exclusively shared by the peroxy oxygen atoms, as in the superoxide O_2^- ion. The present paramagnetic center could not have been observed at room temperature if the hole were localized fully on the central metal atom, i.e. on Nb, converting the Nb(V) into Nb(VI). Hence, the presence of the peroxy ligand has helped in the stability and identification of the radical at room temperature. The above reasoning is further supported by the EHMO calculations done on the DPPN system.

The small ^{93}Nb hyperfine coupling constant arises via spin polarization of the $(\text{O}_1\text{-O}_2)\text{-Nb}$ bond. The perturbation due to quadrupole interaction has been inferred via its effect on the allowed transitions. The forbidden transitions are weak and unresolved due to the large inherent line widths. ENDOR experiments on the DPPN system will be useful in understanding the nature of the interaction present and in independently obtaining the quadrupole coupling constants. Also, the EPR spectra below 77 K might lead to the resolution of different sites and throw further light upon the niobium center present in the system, but this could not be done due to lack of facilities.

Acknowledgment. R.G. thanks the IIT, Madras, for allowing her to pursue research on a part-time basis. P.S.R. thanks the CSIR, India, for a fellowship.

Registry No. DPPN, 12357-41-4; $[\text{NbO}_2\text{F}_3]^-$, 31727-99-8.

Supplementary Material Available: Isofrequency plots in bc^* and ab planes (Figures S1 and S2), bond distances and bond angles in $[\text{NbO}_2\text{F}_3]^{2-}$ (Table S2), anisotropic temperature factors for atoms in DPPN (Table S3), least-squares planes of the anion (Table S4), and input parameters for EHMO calculations on the $[\text{NbO}_2\text{F}_3]^{2-}$ system (Table S5) (6 pages); observed and calculated structure factors for DPPN (Table S1) (5 pages). Ordering information is given on any current masthead page.

Contribution from the Department of Chemistry, University of Otago, P.O. Box 56, Dunedin, New Zealand

Reactions of Coordinated Imidazole. Oxidation Products and Ring Cleavage in the Reactions of RImH^{3+} ($\text{R} = (\text{NH}_3)_5\text{Co}$) with CH_3COOBr and HOBr

Allan G. Blackman, David A. Buckingham,* Charles R. Clark, and Jim Simpson

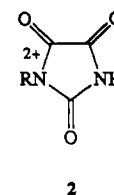
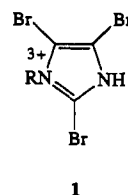
Received August 27, 1990

Treatment of RImH^{3+} ($\text{R} = (\text{NH}_3)_5\text{Co}$, ImH = imidazole) with aqueous Br_2 in acetate (or phosphate) buffer at pH 4-6 results in $\text{R}(\text{parabonate})^{2+}$ (**2**) as the only product (parabonate = imidazolidine-2,4,5-trione). A crystal structure of $[\text{R}(\text{parabonate})]\text{Cl}_2 \cdot 3\text{H}_2\text{O}$ (orthorhombic, $P2_12_12_1$; $a = 6.936$ (1), $b = 11.032$ (3), $c = 19.652$ (3) Å; $Z = 4$; $R = 0.0491$, 1301 reflections) is reported. Formation of **2** appears to occur via initial reaction with $\text{Br}_2(\text{aq})$ to give $\text{R}4,5\text{-Br}_2\text{ImH}^{3+}$ and $\text{R}2,4,5\text{-Br}_3\text{Im}^{2+}$ (**1**), followed by further bromination at C-2 by AcOBr to give a tetrabromo species (**4**), which rapidly hydrolyses. The same product results from oxidation by $\text{Cl}_2(\text{aq})$ in the absence of acetate buffer. Treatment of RImH^{3+} with HOBr in aqueous solution results in three main products. These were identified as $\text{R}(\text{C}_2\text{N}_2\text{H}_3\text{O}_2)^{2+}$ (**7**) containing (probably) the N-coordinated conjugate base of dioxamide, $\text{RN}(\text{CHO})_2^{2+}$ (**11**) containing the N-coordinated conjugate base of diformamide, and $\text{R}(\text{C}_3\text{N}_2\text{O}_3\text{H}_3)^{2+}$ (**12**) containing N-coordinated 2-hydroxyimidazolidine-4,5-dione. A crystal structure of $[\text{R}(2\text{-hydroxyimidazolidine-4,5-dione})](\text{CF}_3\text{SO}_3)_2$ (monoclinic, $C2/m$; $a = 32.325$ (20), $b = 8.037$ (4), $c = 7.195$ (5) Å; $\beta = 91.92$ (5)°; $Z = 4$; $R = 0.0951$, 1348 reflections) is reported.

Introduction

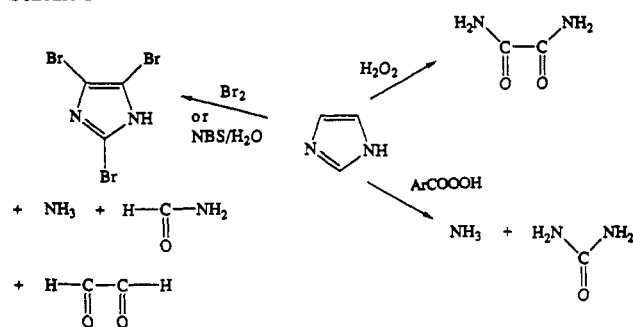
The present experiments arose out of attempts to define the reaction sequence when RImH^{3+} ($\text{R} = (\text{NH}_3)_5\text{Co}$) is treated with Br_2 in aqueous solution.¹ When the reaction is carried out under

reasonably acidic conditions ($[\text{H}^+] \geq 0.01$ M), one of the products, $\text{R}2,4,5\text{-Br}_3\text{ImH}^{3+}$ (**1**) loses (slowly) its imidazole ligand by hy-

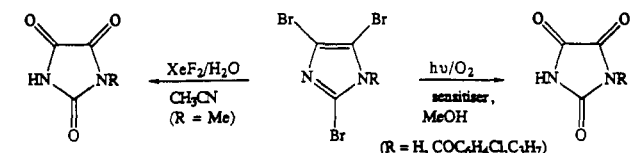


(1) All three sites are successively brominated according to the scheme $\text{RImH}^{3+} \rightarrow \text{R}4\text{-BrImH}^{3+} \rightarrow \text{R}4,5\text{-Br}_2\text{ImH}^{3+} \rightarrow \text{R}2,4,5\text{-Br}_3\text{ImH}^{3+}$; cf.: Blackman, A. G.; Buckingham, D. A.; Clark, C. R.; Kulkarni, S. *Aust. J. Chem.* 1986, 39, 1465. See also: Blackman, A. G.; Buckingham, D. A.; Clark, C. R. *J. Am. Chem. Soc.*, in press.

Scheme I

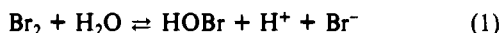


Scheme II



drololysis,² and this complicates chromatographic identification and quantification of the immediate reaction products. However, when the reaction is carried out at pH \sim 4, the bromination reaction is more rapid, and the brominated products are more stable. However, another complication then arises. To maintain constant pH for kinetic reasons, a buffer is normally used (the reaction with Br₂ liberates H⁺), and when this is either acetate or phosphate, another, distinctly different, reaction occurs. The product of the reaction turns out to be the fully oxidized form of coordinated imidazole, **2** (the ligand is known as parabanic acid).³

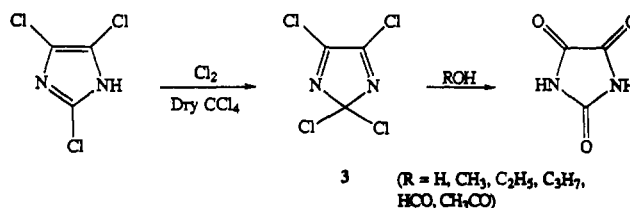
Could this result from oxidation by HOBr? If so, then this reaction (eq 1) would contribute to the first order in [OH⁻] rate law observed at these pHs and previously attributed to the



OH⁻-catalyzed decomposition of the Wheland intermediate formed by addition of Br₂ to RImH³⁺.⁴ Also, HOBr becomes increasingly important in bromine solutions as the pH is raised (eq 1, $K = 5.50 \times 10^{-9} \text{ mol}^2 \text{ kg}^{-2}$),⁵ and it is a somewhat more potent oxidizing agent than Br₂(aq) ($E^\circ = 1.59$ vs 1.09 V). We therefore embarked on a more detailed study of the reaction of RImH³⁺ with Br₂ in the presence of acetate buffer at pH \sim 4, as well as of its reaction with HOBr. It will be seen below that these two reactions result in very different products.

Some background on previous studies concerning oxidations of imidazole is in order. Imidazole itself is reasonably resistant to oxidation, being attacked only by strong oxidizing agents such as MnO₄⁻, H₂O₂, and various peracids.⁶ These reactions usually result in ring degradation, leading to ammonia or ammonia derivatives and aliphatic carbonyl compounds⁵⁻⁷ (Scheme I). Ring degradation has also been observed in halogenations, with imidazole or its 4-substituted derivatives giving a variety of products (cf. Scheme I) when treated with bromine or *N*-bromosuccinimide.⁸ Direct introduction of a carbonyl group without associated ring cleavage is difficult and appears to require the presence of electron-withdrawing substituents. Examples include the pho-

Scheme III



tooxidation of 2,4,5-tribromoimidazoles to parabanic acid⁹ and the reaction of 2,4,5-tribromo-1-methylimidazole with XeF₂¹⁰ (Scheme II), the latter reaction being thought to occur via initial fluorination, followed by hydrolysis.¹¹

The easiest way of obtaining parabanic acid however appears to be via 2,2,4,5-tetrachloro-2*H*-imidazole (**3**), prepared by treating 2,4,5-trichloroimidazole with Cl₂ in dry CCl₄¹² (Scheme III). This species spontaneously, and rapidly, forms parabanic acid on treatment with a wide variety of hydroxylic reagents. The identity of **3** has been confirmed by ¹³C NMR and ³⁵Cl NQR spectroscopy.¹² Its bromo analogue is suggested as an intermediate in this paper.

Experimental Section

General Methods. All reagents were LR or AR grade. Solutions of aqueous bromine were standardized by using excess sodium iodide and titration of the liberated iodine with standard sodium thiosulfate. IR spectra were recorded on a Perkin-Elmer 1600 FT-IR spectrophotometer, and ¹H and ¹³C NMR spectra on a Varian VXR 300 spectrometer (25.0 °C). RP-HPIP chromatography was carried out by using equipment previously described.¹ 2+ complexes were analyzed by using 25 mM sodium 1-hexanesulfonate as the ion-pairing reagent, and mixtures of 2+ and 3+ complexes by using 25 mM sodium dibutyl phosphate, as described.¹ pH-stat rate data were obtained by using a Radiometer TTT60 titrator and a Radiometer ABU12 autoburet in conjunction with a pH electrode assembly.

Preparations. The RImH³⁺, R4,5-Br₂ImH³⁺, and R2,4,5-Br₃Im²⁺ complexes as their bromide or perchlorate salts were prepared as described.¹ When necessary, bromide salts were converted to chloride salts by grinding with AgCl in a little water, and perchlorate salts to chloride salts by using IRA Dowex ion-exchange resin.

[Co(NH₃)₅(parabanate)]Cl₂·3H₂O (**2**). [Co(NH₃)₅ImH]Br₃ (**2**) in a solution of acetate buffer (110 cm³, 0.5 M in NaOAc, 0.25 M in HClO₄) was treated with aqueous bromine (88 cm³, 0.1 M). Testing with starch-iodide paper indicated the very rapid (seconds) consumption of bromine. The reaction mixture was diluted to 2 dm³ with water and sorbed onto a column of Sephadex SP-C25 cation-exchange resin, and the column was washed with water and 0.1 M CF₃COOH. On elution with 0.5 M CF₃COOH, the desired product separated as a red-orange band eluting ahead of the major orange band containing brominated products. The former was collected, loaded onto a short Dowex 50W×2 cation-exchange column, washed with 1 M HCl, and eluted with 3 M HCl. The eluate was taken to dryness (Rotavap) and the product crystallized from water by addition of LiCl (200 mg, 12%). Anal. Calcd (found) for CoC₃H₁₆N₇Cl₂O₃·3H₂O: C, 9.4 (9.2); H, 5.8 (5.8); N, 25.7 (25.4); Cl, 18.6 (18.7). ¹³C NMR (D₂O): δ 173.8, 166.1, 162.2. Electronic spectrum (ε (λ_{max}, nm); 0.01 M HClO₄): 60.4 (483). IR (KBr disk): ν_{C=O} 1802 (w), 1747 (w), 1686 (s). The crystal used in the X-ray study was obtained by slow crystallization of the chloride salt from a ZnCl₂/HCl solution.

[Co(NH₃)₅(2-hydroxyimidazolidine-4,5-dione)]Cl₂·1.5H₂O (**12**), [Co(NH₃)₅N(CHO)₂S₂O₆] (11), and [Co(NH₃)₅C₂N₂H₃O₂](ClO₄)₂ (**7**). A solution of HOBr was prepared by adding ice cold aqueous AgClO₄ (100 cm³, 2 M) to a solution of aqueous bromine (833 cm³, 0.12 M) at 0 °C. The precipitated AgBr was rapidly removed, and the ice cold, faintly yellow solution was immediately added to a solution of [Co(NH₃)₅ImH](ClO₄)₃ (10.2 g) in water (250 cm³) at 0 °C. This was stored at 0 °C for 30 min, during which time further AgBr slowly precipitated. Aqueous phenol (160 cm³, 1 M) and aqueous NaCl (150 cm³, 1 M) were then added to remove excess HOBr and Ag⁺, respectively.

- (2) This hydrolysis reaction is H⁺-catalyzed; c.f.: Blackman, A. G.; Buckingham, D. A.; Clark, C. R. *Inorg. Chem.* To be submitted for publication.
- (3) Biltz, H.; Schiemann, G. *Ber. Dtsch. Chem. Ges.* **1926**, *59*, 721.
- (4) Blackman, A. G.; Buckingham, D. A.; Clark, C. R. *Inorg. Chem.* Submitted for publication.
- (5) Ramette, R. W.; Palmer, D. A. *J. Soln. Chem.* **1986**, *15*, 387.
- (6) Grimmett, M. R. In *Comprehensive Heterocyclic Chemistry*; Katritzky, A. R., Rees, C. W., Eds.; Pergamon: Oxford, England, 1984, Vol. 5, Part 4A, p 405.
- (7) Schofield, K.; Grimmett, M. R.; Keene, B. R. T. In *Heterocyclic Nitrogen Compounds: The Azoles*; Cambridge Univ. Press: Cambridge, England, 1976; p 126.
- (8) Schmir, G. L.; Cohen, L. A. *Biochemistry* **1965**, *4*, 533.

- (9) Wamhoff, H.; Abdou, W. M.; Zahran, M. *J. Agric. Food Chem.* **1988**, *36*, 205.
- (10) Nikolenko, L. N.; Tolmacheva, N. S.; Shustov, L. D. *J. Gen. Chem. USSR (Engl. Transl.)* **1979**, *49*, 1251.
- (11) It is not stated in ref 10 whether or not fluoro derivatives can be isolated in the absence of moisture.
- (12) Büchel, K. H.; Erdmann, H. *Chem. Ber.* **1976**, *109*, 1625.

The precipitate was removed. The solution was diluted to 4 dm³ with water and sorbed onto a column of Sephadex SP-C25 cation-exchange resin, which was washed with water followed by 0.1 M NaClO₄. On elution with 0.4 M NaClO₄, the product mixture separated as a deep orange band (75%) ahead of a red-orange band of [Co(NH₃)₃OH₂]²⁺ (25%). The former was collected and the volume reduced by rotary evaporation until [Co(NH₃)₃C₂N₂H₃O₂](ClO₄)₂ crystallized. This was removed, and on further concentration of the solution, impure [Co(NH₃)₃N(CHO)₂](ClO₄)₂ crystallized. This was removed, and the filtrate containing [Co(NH₃)₃(2-hydroxyimidazolidine-4,5-dione)]²⁺ was diluted and sorbed onto a column of Sephadex SP-C25 cation-exchange resin. The column was washed with water and 0.1 M CF₃COOH, and the orange band eluted with 0.5 M CF₃COOH. Rotary evaporation to dryness and recrystallization as the chloride salt by adding LiCl to a concentrated aqueous solution gave the complex as orange microcrystals. Anal. Calcd (found) for CoC₃H₁₈N₇Cl₂O₃·1.5H₂O: C, 10.1 (10.2); H, 5.9 (5.9); N, 27.5 (27.5); Cl, 19.9 (20.2). ¹H NMR (D₂O): δ 5.78 (s, 1 H). ¹³C NMR (D₂O): δ 172.3, 162.4, 87.5. Electronic spectrum (ε (λ_{max}, nm); 0.01 M HClO₄): 71.1 (488). Orange platelike crystals of [Co(NH₃)₃(2-hydroxyimidazolidine-4,5-dione)](CF₃SO₃)₂ suitable for the X-ray study were obtained by adding sodium triflate to a warm, concentrated solution of the trifluoroacetate salt and slowly cooling.

[Co(NH₃)₃N(CHO)₂](ClO₄)₂ (11) was purified as follows. The crude solid was dissolved in the minimum amount of hot water and NaClO₄ added to precipitate the [Co(NH₃)₃C₂N₂H₃O₂](ClO₄)₂ impurity. This was removed and the filtrate reduced to dryness (Rotavap). Crystallization from warm water by adding Na₂S₂O₆ and cooling on ice afforded the product as orange microcrystals. Anal. Calcd (found) for CoC₂H₁₇N₆S₂O₈: C, 6.4 (6.4); H, 4.6 (4.6); N, 22.3 (22.0); S, 17.0 (16.8). ¹H NMR (D₂O): δ 8.73 (s, 2 H). ¹³C NMR (D₂O): δ 184.1. Electronic spectrum (ε (λ_{max}, nm); water): 53.6 (487).

[Co(NH₃)₃C₂N₂H₃O₂](ClO₄)₂ (7) was purified by recrystallization (3×) of the crude solid from hot water by adding NaClO₄ and cooling in ice. Anal. Calcd (found) for CoC₂H₁₇N₇Cl₂O₁₀: C, 5.6 (6.0); H, 4.2 (4.2); N, 22.8 (23.6); Cl, 16.5 (17.2). ¹³C NMR (D₂O): δ 154.0, 112.1. Electronic spectrum (ε (λ_{max}, nm); 0.01 M HClO₄): 73.8 (482), 81.7 (347). This complex was also obtained as the chloride salt by adding LiCl to a hot concentrated aqueous solution of the perchlorate salt and cooling in ice. Anal. Calcd (found) for CoC₂H₁₈N₇Cl₂O₂: C, 8.0 (8.0); H, 6.0 (5.8); N, 32.5 (32.3); Cl, 23.5 (23.9).

[Co(NH₃)₃NCO](ClO₄)₂ was prepared by an adaptation of the method of Balahura and Jordan¹³ by heating [Co(NH₃)₃OH₂](ClO₄)₃ (10 g) and urea (10 g) in trimethyl phosphate (80 cm³) on a water bath over molecular sieves (3 Å, 5 g) for 1 h. The solution was cooled and filtered, and the product was precipitated by addition of 2-butanol (500 cm³). The crude product was twice recrystallized from warm water by adding NaClO₄ and cooling in ice (1.8 g, 22%). Anal. Calcd (found) for CoCH₁₅N₆Cl₂O₉: C, 3.1 (3.1); H, 3.9 (3.8); N, 21.8 (21.9); Cl, 18.4 (18.4). ¹³C NMR (D₂O): δ 128.3. Electronic spectrum (ε (λ_{max}, nm); water): 126 (501), 82.1 (354). Isolation as the chloride salt was achieved by crystallization (2×) from hot water by adding LiCl and cooling in ice. Electronic spectrum (ε (λ_{max}, nm); water): 113 (501), 75.2 (354). IR (KBr disk): ν_{NCO} 2264, 1305 cm⁻¹.

Alkaline Hydrolysis of [Co(NH₃)₃C₂N₂H₃O₂]²⁺ (7). To a solution of [Co(NH₃)₃C₂N₂H₃O₂](ClO₄)₂ (150 mg) in water (10 cm³) was added aqueous NaOH (25 cm³, 0.03 M). Addition of LiCl and cooling in ice gave a red-orange precipitate of [Co(NH₃)₃NCO]Cl₂, which was crystallized from hot water by addition of LiCl (100 mg). Anal. Calcd (found) for CoCH₁₅N₆Cl₂O: C, 4.7 (4.6); H, 5.9 (6.0); N, 32.7 (32.7); Cl, 27.6 (27.3). ¹³C NMR (D₂O): δ 129.1. Electronic spectrum (ε (λ_{max}, nm); water): 117 (501), 76.4 (353). IR (KBr disk): ν_{NCO} 2263, 1305 cm⁻¹ (identical with an authentic sample of [Co(NH₃)₃NCO]Cl₂).

pH-Stat Alkaline Hydrolysis of [Co(NH₃)₃C₂N₂H₃O₂]²⁺ (7). A solution of the complex (74.13 mg) in aqueous NaCl (3.00 cm³, 1 M) in a thermostated beaker was rapidly adjusted to pH 11.50 by using 1 M NaOH (0.045 cm³). The pH was maintained at this value (pH-stat), and a further 0.206 cm³ of 1 M NaOH was found to be consumed during hydrolysis. The rate of OH⁻ consumption was monitored at 25.0 °C. The very insoluble [Co(NH₃)₃NCO]Cl₂ complex precipitated during the reaction.

Acid-Catalyzed Hydrolysis. To a solution of [Co(NH₃)₃C₂N₂H₃O₂](ClO₄)₂ in water was added sufficient aqueous NaOH to ensure the final pH was ~12. After reaction had ceased, the solution was acidified (pH 1) with HClO₄ and the resulting orange solution reduced to dryness (Rotavap). Crystallization from hot water by adding NaClO₄ and cooling in ice gave the product as golden microcrystals. Its infrared spectrum was identical with that of authentic [Co(NH₃)₃](ClO₄)₃.¹⁴

Table I. Crystal Data and Data Collection and Refinement Parameters for Compounds 2 and 12

	compd 2	compd 12
Crystal Data		
empirical formula	C ₃ H ₂₂ O ₆ N ₇ Cl ₂ Co	C ₃ H ₁₆ N ₇ O ₉ F ₆ S ₂ Co
fw	382.09	555.28
cryst system	orthorhombic	monoclinic
space group	P2 ₁ 2 ₁ 2 ₁ (No. 19) ^a	C2/m (No. 12) ^a
a, Å	6.936 (1)	32.325 (20)
b, Å	11.032 (3)	8.037 (4)
c, Å	19.652 (3)	7.195 (5)
β, deg		91.92 (5)
V, Å ³	1503.8 (5)	1868 (3)
D _c , g cm ⁻³	1.69	1.97
Z	4	4
cryst size, mm	0.8 × 0.4 × 0.08	0.15 × 0.11 × 0.07
μ(Mo Kα), cm ⁻¹	15.73	12.96
F(000)	792	1120
Data Collection and Refinement Parameters		
diffractometer	Nicolet R3M	Nicolet R3M
temp, K	293 ± 5	153 ± 5
radiation (λ, Å)	Mo Kα (0.710 69)	Mo Kα (0.710 69)
scan type	ω - 2θ	ω - 2θ
scan speed, deg min ⁻¹	15.00	4.88
data limits, deg	4 < 2θ < 52	5 < 2θ < 52
reflens measd	h, k, l	h, k, ±l
cryst decay, %	< 2 ^b	< 2 ^b
abs cor	empirical ^c	empirical ^c
transm	0.979 (max)	0.666 (max)
	0.635 (min)	0.619 (min)
total no. of obsd data	1802 ^c	2002 ^c
no. of unique data	1301 (I > 2σ(I))	1308 (I > 2σ(I))
no. of variables	196	175
R (ΣΔF/Σ F _o)	0.0491	0.0951
R _w [Σw ^{1/2} (ΔF)/Σw ^{1/2} F _o]	0.0596	0.1034
weight (w)	0.4368/(σ ² F + 0.0006F ²)	2.0610/(σ ² F + 0.004238F ²)

^a International Tables for X-ray Crystallography; Kynoch Press: Birmingham, England, 1966; Vol. I. ^b Standard reflections (400), (060), and (008) for compound 2 and (12,0,0), (040), and (003) for compound 12 measured after every 100 reflections. ^c Lorentz and polarization corrections and empirical absorption corrections were applied by using the SHELXTL system.¹⁶

Formation of Parabanic Acid from 2,4,5-Tribromoimidazole. To a suspension of 2,4,5-tribromoimidazole in phosphate buffer (D₂O) in an NMR tube was added Br₂ in D₂O (1 mol equiv). On shaking of the tube, the solid slowly dissolved, and the bromine color disappeared to give a colorless solution. ¹³C NMR spectroscopy showed two peaks at low field (δ 161.7, 156.4) of approximate intensity ratio 2:1, consistent with the reported spectrum of parabanic acid (Me₂SO-d₆: δ 159.7, 154.6).¹⁵

Kinetic Data. These were collected on a Cary 219 spectrophotometer (25.0 °C) as follows.

Alkaline Hydrolysis of [Co(NH₃)₃C₂N₂H₃O₂]²⁺. To a solution of buffer ([CAPS] = 0.2 M, I = 1.0 M (NaClO₄)) was added an equal volume of a solution of [Co(NH₃)₃C₂N₂H₃O₂](ClO₄)₂ in 1.0 M NaClO₄, and the absorbance increase at 498 nm was monitored. Plots of log (A_t - A_∞) vs time were linear over more than 2 half-lives. The pH was measured at the completion of a run.

Acid Hydrolysis of [Co(NH₃)₃NCO]²⁺. To a solution of HClO₄ (0.2, 0.02 M, I = 2.0 M (NaClO₄)) was rapidly added an equal volume of a solution of [Co(NH₃)₃NCO](ClO₄)₂ in water, and the absorbance decrease at 500 nm was monitored. Plots of log (A_t - A_∞) vs time were linear over more than 2 half-lives.

X-ray Data Collection and Reduction. Compound 2. Crystals of [Co(NH₃)₃(parabanate)]Cl₂·3H₂O were grown as described above, and an orange needle was selected and used for data collection. The unit cell dimensions and orientation matrices were calculated from 25 accurately centered reflections on a Nicolet P3M fully automated diffractometer. Details of the crystal, data collection, and structure refinement are summarized in Table I. Data were processed and empirical absorption corrections applied by using programs from the SHELXTL package.¹⁶

Compound 12. Small orange plates of [Co(NH₃)₃(C₂N₂O₃H₃)](CF₃SO₃)₂ were obtained as described above. Unit cell dimensions were

(13) Balahura, R. J.; Jordan, R. B. *Inorg. Chem.* 1970, 9, 1567.

(14) Prepared by the method of: Schlessinger, G. *Inorg. Synth.* 1967, 9, 160.

(15) Coxon, B.; Fatiadi, A. J.; Sniegowski, H. S.; Hertz, L. T.; Schaffer, R. *J. Org. Chem.* 1977, 42, 3132.

(16) Sheldrick, G. M. SHELXTL. An integrated system for solving, refining, and displaying crystal structures from diffraction data. University of Göttingen, 1981.

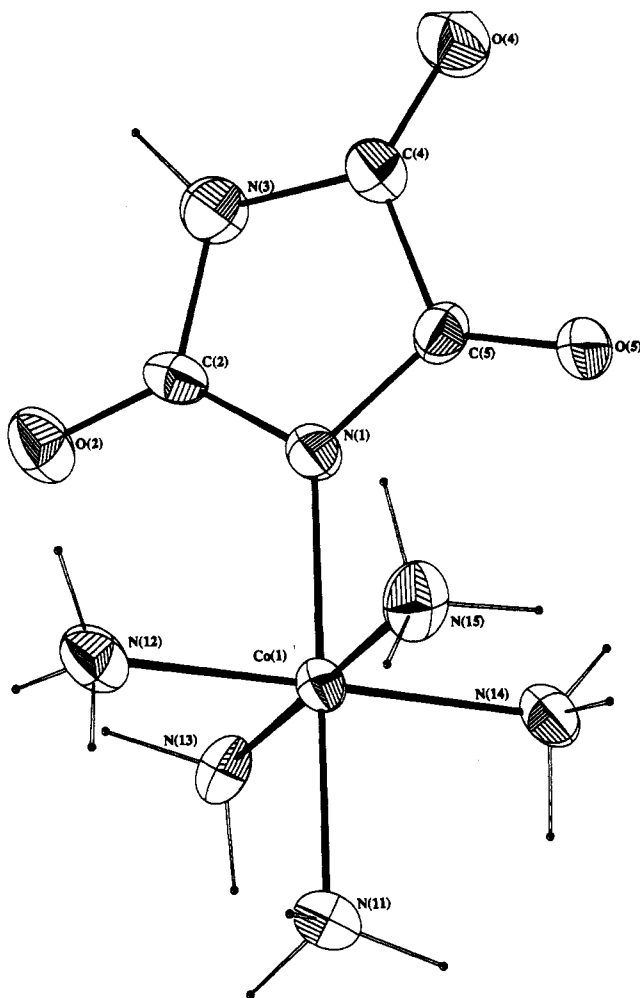


Figure 1. View of the R(parabanate)²⁺ cation, **2**, showing the atom-numbering scheme. Thermal ellipsoids enclose 50% probability levels.

found as described above, and the crystallographic data are detailed in Table I. Systematic absences in the data indicated the monoclinic space groups *C2*, *Cm*, or *C2/m*. Analysis of the *E*-statistics clearly indicated a centrosymmetric structure, and sensible solutions were not obtained in either of the noncentrosymmetric alternatives. The choice of the space group as *C2/m* was vindicated by the success of the structure refinement. The crystals were small and weakly diffracting, but X-ray data obtained at 153 K proved sufficient to solve the structure although the crystal quality together with disorder problems involving the trifluoromethanesulfonate anions (vide infra) led to poor residuals and standard deviations.

Structure Solution and Refinement. Compound **2**. The Patterson search procedure of SHELXTL¹⁶ located the positions of the Co atom and the two Cl⁻ anions; the remaining non-hydrogen atoms were found by successive difference Fourier syntheses and least-squares refinements.¹⁷ All non-hydrogen atoms were assigned anisotropic temperature factors, and a fixed weighting scheme was introduced. A difference Fourier synthesis at this point revealed electron density in appropriate positions and orientations for H atoms. These were included on the ammine ligands, the uncoordinated N(3) atom of the imidazole ring, and the water molecules in calculated positions with $r_{E-H} = 0.98$ Å and fixed isotropic temperature factors. In subsequent refinement cycles the water molecules were refined as rigid groups. This model for the structure converged with $R = 0.0491$ and $R_w = 0.0567$. Refinement to convergence with the signs of all positional coordinates reversed gave $R = 0.0495$ and $R_w = 0.0581$, indicating that the handedness of the structure is more accurately represented by the original coordinates. The final difference Fourier map showed a peak of ~ 1.3 e Å⁻³, located between N(13) and N(14) and approximately 2.00 Å from the Co atom. It is not possible to attach chemical significance to this observation.

Compound 12. The structure was solved by Patterson methods¹⁶ and refined as described above. The hydroxyl O and H substituents on C(2) of the imidazole ring were disordered with respect to the imidazole ring

Table II. Final Positional and Equivalent Thermal Parameters for [(NH₃)₅Co(parabanate)]Cl₂·3H₂O

atom	<i>x/a</i>	<i>y/b</i>	<i>z/c</i>	<i>U</i> _{eq} , Å ²
Co(1)	0.8206 (2)	0.0125 (1)	0.5858 (0)	0.019
N(11)	0.822 (1)	0.0471 (5)	0.6842 (3)	0.032
N(12)	1.026 (1)	0.1304 (6)	0.5748 (4)	0.031
N(13)	0.624 (1)	0.1373 (6)	0.5730 (4)	0.030
N(14)	0.612 (1)	-0.1062 (6)	0.5985 (4)	0.028
N(15)	1.020 (1)	-0.1112 (6)	0.5995 (4)	0.032
N(1)	0.823 (1)	-0.0224 (4)	0.4883 (3)	0.022
C(2)	0.829 (1)	0.0638 (6)	0.4373 (4)	0.024
O(2)	0.829 (1)	0.1727 (4)	0.4444 (3)	0.033
N(3)	0.830 (1)	0.0074 (5)	0.3730 (3)	0.033
C(4)	0.823 (2)	-0.1154 (6)	0.3804 (4)	0.030
O(4)	0.819 (1)	-0.1934 (5)	0.3367 (3)	0.046
C(5)	0.819 (2)	-0.1344 (6)	0.4578 (4)	0.025
O(5)	0.816 (1)	-0.2351 (4)	0.4859 (3)	0.034
Cl(1)	1.3146 (4)	0.0449 (2)	0.7086 (1)	0.036
Cl(2)	1.3282 (5)	0.0689 (2)	0.4485 (1)	0.043
Ow(1)	0.304 (2)	0.8366 (5)	0.3592 (3)	0.065
Ow(2)	0.157 (3)	0.8175 (7)	0.8016 (5)	0.136
Ow(3)	0.801 (4)	0.1683 (7)	0.2630 (4)	0.179

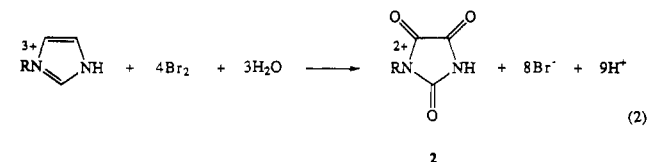
Table III. Bond Lengths and Angles for [(NH₃)₅Co(parabanate)]Cl₂·3H₂O

Bond Lengths (Å)			
Co(1)-N(11)	1.969 (6)	N(1)-C(5)	1.374 (8)
Co(1)-N(12)	1.942 (7)	C(2)-O(2)	1.209 (8)
Co(1)-N(13)	1.955 (6)	C(2)-N(3)	1.408 (9)
Co(1)-N(14)	1.970 (7)	N(3)-C(4)	1.364 (9)
Co(1)-N(15)	1.961 (7)	C(4)-O(4)	1.216 (9)
Co(1)-N(1)	1.955 (6)	C(4)-C(5)	1.53 (1)
N(1)-C(2)	1.383 (9)	C(5)-O(5)	1.241 (8)
Angles (deg)			
N(11)-Co(1)-N(12)	88.6 (3)	N(15)-Co(1)-N(1)	89.4 (3)
N(11)-Co(1)-N(13)	89.6 (3)	Co(1)-N(1)-C(2)	125.1 (4)
N(11)-Co(1)-N(14)	90.5 (3)	Co(1)-N(1)-C(5)	127.3 (4)
N(11)-Co(1)-N(15)	89.9 (3)	C(2)-N(1)-C(5)	107.6 (6)
N(11)-Co(1)-N(1)	179.1 (4)	N(1)-C(2)-O(2)	126.9 (7)
N(12)-Co(1)-N(13)	91.5 (3)	N(1)-C(2)-N(3)	110.2 (6)
N(12)-Co(1)-N(14)	179.1 (3)	O(2)-C(2)-N(3)	122.9 (6)
N(12)-Co(1)-N(15)	88.0 (3)	C(2)-N(3)-C(4)	110.1 (6)
N(12)-Co(1)-N(1)	90.9 (3)	N(3)-C(4)-O(4)	128.9 (8)
N(13)-Co(1)-N(14)	88.3 (3)	N(3)-C(4)-C(5)	104.0 (6)
N(13)-Co(1)-N(15)	179.3 (3)	O(4)-C(4)-C(5)	127.1 (7)
N(13)-Co(1)-N(1)	91.1 (3)	N(1)-C(5)-C(4)	108.0 (5)
N(14)-Co(1)-N(15)	92.2 (3)	N(1)-C(5)-O(5)	127.6 (6)

plane, and the hydroxyl H atom was not included in the final refinement. High and increasing temperature factors for the atoms of the two trifluoromethanesulfonate anions indicated substantial positional disorder. Furthermore, a final difference Fourier synthesis showed peaks of height 1.7–1.2 e Å⁻³ in the vicinity of the anions. The second anion, containing S(2), was particularly ill-defined with unusual S–O and C–F bond distances, but a satisfactory model of the disorder could not be obtained. The final model converged with $R = 0.095$ and $R_w = 0.103$.

Results and Discussion

1. Formation of Coordinated Parabanic Acid. Bromination of RImH³⁺ using excess Br₂ buffered with aqueous sodium acetate (or sodium phosphate) results in R(parabanate)²⁺ (**2**) as the only product. The stoichiometry required by eq 2 was verified by



chromatographic (HPLC) identification and quantitation using 1–4 mol equiv of bromine. **2** was isolated as [Co(NH₃)₅(parabanate)]Cl₂·3H₂O and its identity established by X-ray structural analysis. A representation of the complex cation is shown in Figure 1, which also defines the atom-numbering scheme. Final positional and thermal parameters are given in Table II, and bond lengths and angles are given in Table III. The octahedral cation has the

(17) Sheldrick, G. M. SHELX-76. Program for crystal structure determination. University of Cambridge, 1976.

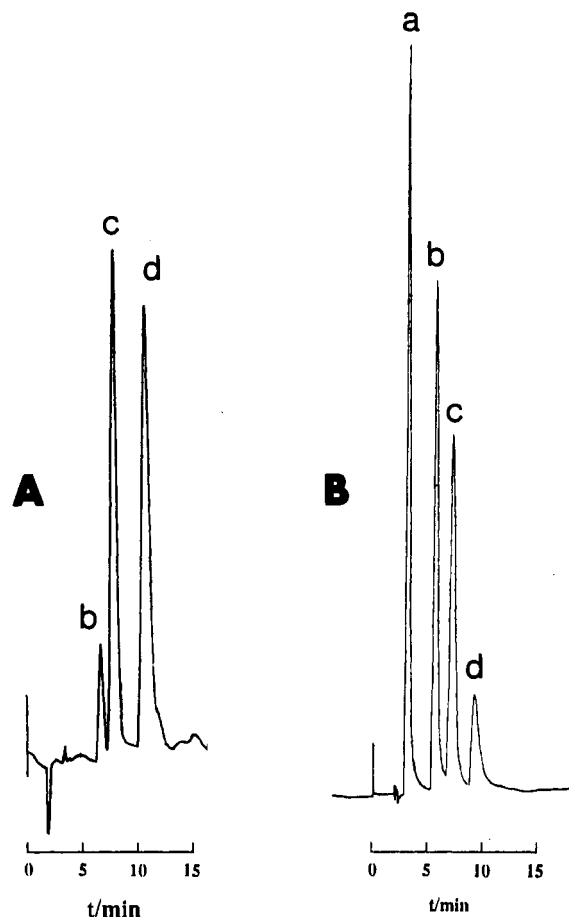
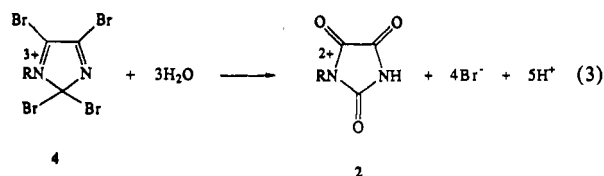


Figure 2. RP-HPIP chromatograms showing the effects of acetate buffer on the products of the reaction of RImH^{3+} with aqueous Br_2 at pH 4.7. (A) Products in the absence of acetate (pH-stat control), using ~ 2 mol equiv of Br_2 . The elution order is unreacted RImH^{3+} (~ 6 min), $\text{R}_{2,4,5}\text{-Br}_3\text{Im}^{2+}$ (~ 8 min), and $\text{R}_{4,5}\text{-Br}_2\text{ImH}^{3+}$ (~ 11 min). (B) Products using ~ 1 mol equiv of Br_2 in half-neutralized 0.1 M acetate buffer. The first peak (~ 3.5 min) represents $\text{R}(\text{parabanate})^{2+}$ (**2**), and the following peaks are as listed in (A). Detection was at 250 nm.

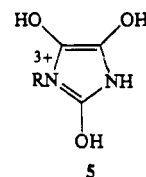
heterocycle coordinated to cobalt through its deprotonated N atom. The heterocycle is planar to within 0.003 Å and approximately bisects the angles between the $\text{N}(1)\text{-N}(11)\text{-N}(12)\text{-N}(14)$ (45.4 (4°)) and $\text{N}(1)\text{-N}(11)\text{-N}(13)\text{-N}(15)$ (46.4 (4°)) mean planes. Comparison of bond lengths and angles of the coordinated ligand with those for uncomplexed parabanic acid¹⁸ shows that coordination has little effect on the structure of the heterocycle. The C–O bond lengths (1.209, 1.216, 1.241 Å; Table III) clearly indicate double bonds and define the ligand as deprotonated parabanic acid rather than its trihydroxyimidazole tautomer. No proton signals appear in the ^1H spectrum, and the three low-field ^{13}C absorptions (173.8, 166.1, 162.2 ppm) have long relaxation times typical of carbonyl carbons. The IR spectrum shows a strong absorption at 1686 cm^{-1} . The complex behaves as a $2+$ cation on chromatography, eluting close to the solvent front and before any imidazole complex (Figure 2).

Compound **2** is also formed when $\text{R}_{4,5}\text{-Br}_2\text{ImH}^{3+}$ or $\text{R}_{2,4,5}\text{-Br}_3\text{Im}^{2+}$ (**1**) is treated with Br_2 in acetate buffer. Both of these reactions are fast (seconds), and 1 mol equiv of Br_2 was found to be sufficient for the complete conversion of **1**. This suggests oxidation of RImH^{3+} occurs via **1** with further bromination at C-2 giving **4**, followed by spontaneous hydrolysis (eq 3).

The reaction resembles chlorination of the free ligand in nonaqueous solution (cf. Scheme III).¹² However acetate (or phosphate) is a necessary ingredient in the present instance. Thus, addition of 2 mol equiv of Br_2 to RImH^{3+} at pH 4.7 in the absence



of buffer (pH-stat) gave only di- and tribrominated products in addition to some unreacted RImH^{3+} (Figure 2A). Likewise **1** reacts, only very slowly, by hydrolysis (to give ROH_2^{3+} and 2,4,5-tribromoimidazole)² in phosphate or acetate buffer at pH 4.7 in the absence of Br_2 . Thus, hydrolysis of **1** to give **5** does



not occur as an initial step. It was also shown that parabanic acid can be directly formed by treating the uncoordinated ligand 2,4,5-tribromoimidazole with Br_2 in an aqueous solution containing phosphate buffer. Thus, the reaction is not restricted to its $(\text{NH}_3)_5\text{Co}^{3+}$ complex, but it is faster for this species.

The amount of **2** formed depends both on the total amount of buffer present and on the concentration of its basic component. This is shown by the two chromatographic sequences given in Figure 3. Figure 3A shows that decreasing amounts of total acetate gives less **2** and increasing amounts of $\text{R}_{2,4,5}\text{-Br}_3\text{Im}^{2+}$ and $\text{R}_{4,5}\text{-Br}_2\text{ImH}^{3+}$. Figure 3B shows that decreasing OAc concentration at constant total acetate gives a similar result. Significantly, the amount of RImH^{3+} left unreacted remains essentially constant in the two experiments, and it has previously been shown that acetate buffer does not catalyze the reaction of Br_2 with RImH^{3+} at pH ~ 4 .¹ This suggests that the acetate-catalyzed reaction is faster than initial mono- or dibromination. Also, both chromatographic sequences suggest that **2** is directly formed from both $\text{R}_{2,4,5}\text{-Br}_3\text{Im}^{2+}$ and $\text{R}_{4,5}\text{-Br}_2\text{ImH}^{3+}$, since the amounts of both species decrease with increasing $[\text{OAc}^-]$.

Other non-halogen-containing oxidizing agents such as H_2O_2 ($E^\circ = 1.78\text{ V}$) and MnO_4^- ($E^\circ = 1.49\text{ V}$), both stronger oxidizing agents than Br_2 ($E^\circ = 1.09\text{ V}$) and of comparable power to HOBr ($E^\circ = 1.59\text{ V}$), gave no reaction (HPIPC) when added to aqueous acidic solutions of **1**. Thus, the process is not simply one of oxidation. However, treating RImH^{3+} with an aqueous solution of Cl_2 in the absence of buffer gives an immediate reaction, from which **2** was isolated and identified.

Such pieces of evidence require **2** to be formed by strong halogen-containing oxidants. Aqueous Cl_2 suffices, but aqueous Br_2 is not strong enough. Initial halogenation by Br_2 seems to occur, at least to the $\text{R}_{4,5}\text{-Br}_2\text{ImH}^{3+}$ stage. Subsequent reaction of $\text{R}_{4,5}\text{-Br}_2\text{ImH}^{3+}$ and $\text{R}_{2,4,5}\text{-Br}_3\text{Im}^{2+}$ requires OAc^- ion in addition to Br_2 . This suggests acetyl hypobromite, CH_3COOBr , as the active oxidizing agent. CH_3COOBr is known to be a good source of Br^+ in acetic acid (better even than Br_2),¹⁹ and in aqueous solutions similar to the present one it is the likely catalyst in the rapid oxidations of dimethyl sulfoxide to dimethyl sulfone²⁰ and of $\text{Co}(\text{III})$ -chelated methionine sulfoxide to methionine sulfone.²¹ Both reactions probably occur via initial bromination at sulfur, followed by hydrolysis. In the present case further bromination at C-2 would give **4**, which then rapidly hydrolyses in the aqueous environment to **2** (Scheme IV). An alternative, but we feel less likely, mechanism, in view of the reactions with HOBr to be described below, is AcO^- -catalyzed nucleophilic attack by HOBr to give the trihypobromite derivative **6** (Scheme V), which then undergoes Br^- -induced degradation liberating 2 mol of Br_2 and **2**.

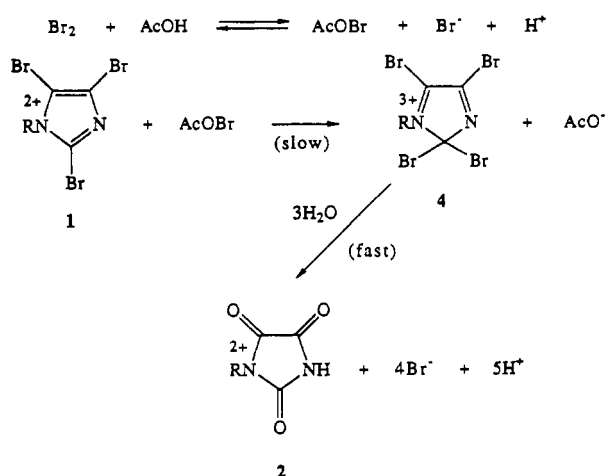
(19) de la Mare, P. B. D.; Maxwell, J. L. *J. Chem. Soc.* **1962**, 4829.

(20) Cox, B. G.; Gibson, A. *J. Chem. Soc. Perkin Trans. 2* **1973**, 1355.

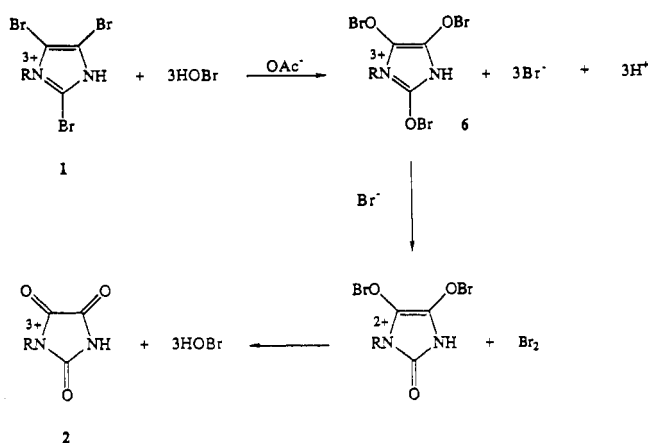
(21) Sutton, P. A. Unpublished work, Ph.D. Thesis, University of Otago, 1988; Chapter 2, p 35.

(18) Craven, B. M.; McMullan, R. K. *Acta Crystallogr., Sect. B* **1979**, *B35*, 934.

Scheme IV



Scheme V



2. Reaction with HOBr. Addition of a freshly prepared ice-cold solution of HOBr (containing excess AgClO_4) to aqueous RImH^{3+} gives an immediate orange to orange-red color change. Chromatography (HPIPC) following the addition of 1.7 mol equiv gave a 2+ ion eluting prior to unreacted starting material, which was followed by two very much smaller peaks with retention times characteristic of $\text{R}_{2,4,5}\text{-Br}_3\text{Im}^{2+}$ and $\text{R}_{4,5}\text{-Br}_2\text{ImH}^{3+}$. Addition of 8 mol equiv of HOBr gave quantitative formation of the 2+ band. Preparative chromatography using SP-C25 cation-exchange resin and aqueous NaClO_4 as eluent gave a broad red 2+ band containing three species. These were separated and characterized as described below.

(i) $\text{R}(\text{C}_2\text{N}_2\text{H}_3\text{O}_2)^{2+}$. $[\text{Co}(\text{NH}_3)_5(\text{C}_2\text{N}_2\text{H}_3\text{O}_2)](\text{ClO}_4)_2$ crystallized on reducing the solution volume. Repeated recrystallization failed to remove traces of a faster moving (HPIPC) 2+ impurity, but conversion to the chloride salt (ion exchange) and further recrystallization gave a chromatographically pure product that was characterized analytically as its chloride salt. Addition of LiBr to a hot concentrated solution of this material and cooling produced well-formed orange octahedral crystals, but X-ray data suggested ligand disorder over at least two coordination sites and the structure could not be solved.

^1H NMR spectroscopy showed no proton signals apart from ammine protons, and exchange of these (addition of Na_2CO_3 to D_2O solution) confirmed that the ammine signal did not obscure any nonexchangeable C-H protons. The ^{13}C spectrum gave two absorptions (112.1 and 154.0 ppm), with the high-field signal significantly broadened, suggesting rapid exchange at this site. The IR spectrum showed a broadish asymmetric band centered at 1647 cm^{-1} (but probably consisting of a broad signal at $\sim 1600\text{ cm}^{-1}$ and a sharp peak at $\sim 1650\text{ cm}^{-1}$) and a sharp absorption at 1228 cm^{-1} , in addition to signals due to $\text{Co}(\text{NH}_3)_5$ and adventitious water. The visible spectrum has a maximum at 482

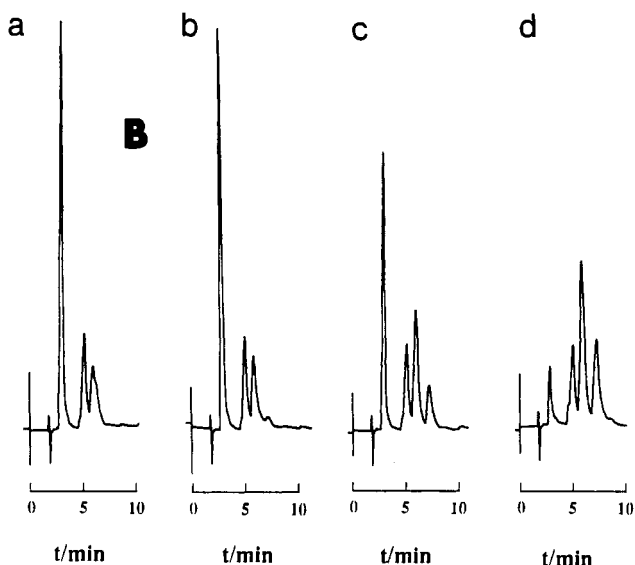
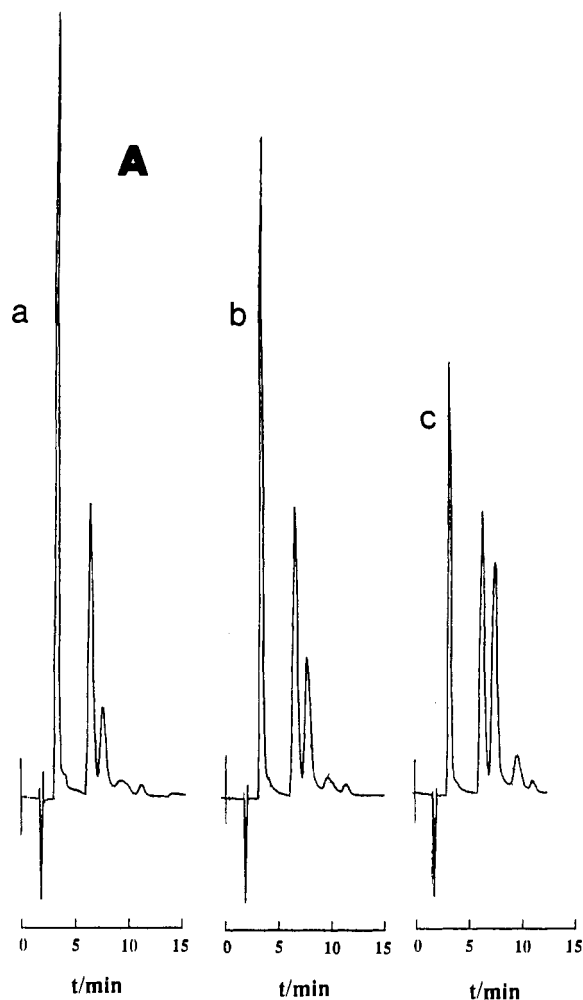


Figure 3. RP-HPIPC chromatograms showing the effects of increasing total acetate, and increasing OAc^- concentration at constant total acetate, on the products of the reaction of RImH^{3+} with Br_2 at pH 4.7. (A) Sequence representing $[\text{acetate}]_{\text{T}} = 0.40\text{ M}$ (a), 0.20 M (b), and 0.10 M (c) (~ 3.5 min), RImH^{3+} (~ 6.5 min), $\text{R}_{2,4,5}\text{-Br}_3\text{Im}^{2+}$ (~ 7.5 min), $\text{R}_{4,5}\text{-Br}_2\text{ImH}^{3+}$ (~ 9 min), and ROH_2^{3+} (~ 11 min), the latter resulting from some hydrolysis of $\text{R}_{2,4,5}\text{-Br}_3\text{Im}^{2+}$. (B) Sequence representing (a) HOAc (0.04 M)/NaOAc (0.17 M), (b) HOAc (0.105 M)/NaOAc (0.105 M), (c) HOAc (0.17 M)/NaOAc (0.04 M), and (d) HOAc (0.21 M)/NaOAc (none). The elution order is as given in (A). Detection was at 250 nm .

Table IV. Rate Data for the Alkaline Hydrolysis of $[(\text{NH}_3)_5\text{CoC}_2\text{N}_2\text{H}_2\text{O}_2]\text{Cl}_2$ at 25.0 °C, $I = 1.0 \text{ M}$ (NaClO_4)^a

pH	$10^4 k, \text{ s}^{-1}$	$k_{\text{OH}}, \text{ M}^{-1} \text{ s}^{-1}$ ^b
10.14	0.46	0.20
10.63	1.30	0.18
11.11	3.73	0.17

^a $[\text{Co}]_{\text{T}} \sim 1.0 \text{ mM}$; 0.2 M CAPS buffer. ^b $k_{\text{OH}} = k/[\text{OH}^-]$; $\text{p}K_{\text{w}} = 13.77$ (1 M NaClO_4).

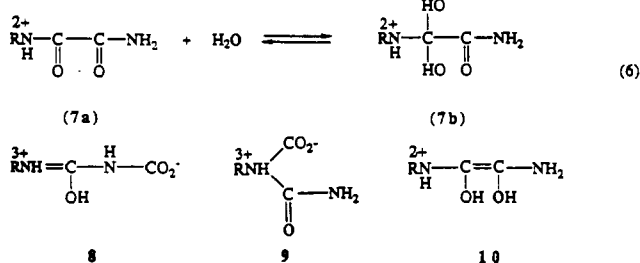
nm characteristic of a CoN_6 chromophore, and this spectrum remained unchanged in 3 M HClO_4 .

Alkaline hydrolysis gave a quantitative yield of the cyanato complex $[\text{Co}(\text{NH}_3)_5\text{NCO}]^{2+}$, and 1 mol equiv of OH^- was consumed in the process (eq 4). Isolated $[\text{Co}(\text{NH}_3)_5\text{NCO}]\text{Cl}_2$ was

$$\text{RC}_2\text{N}_2\text{H}_3\text{O}_2^{2+} + \text{OH}^- \rightarrow \text{RNCO}^{2+} + \text{CNO}_3\text{H}_4(\text{H}_2\text{O})_x^- \quad (4)$$

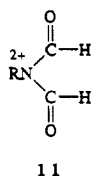

characterized by elemental analysis, by ^{13}C , IR, and visible spectral data, and by the product and rate of formation of RNH_3^{3+} in acid solution (eq 5). Rate data for reaction 4 (Table IV) show a first order in $[\text{OH}^-]$ rate law, $k_{\text{obs}} = k_{\text{OH}}[\text{OH}^-]$, with $k_{\text{OH}} = 0.18 \text{ M}^{-1} \text{ s}^{-1}$ at 25 °C in $I = 1.0 \text{ M}$ NaClO_4 .

Structures 7–10 all show some consistency with the above data, with the gemdiol (7b) being the most consistent with the aqueous



^{13}C data;²² however simple N-coordinated oxamides apparently do not hydrate to any significant extent in water.²³ The coordinated imidic acid structures 8 and 9 would not be expected to have a ^{13}C signal at 112.1 ppm, and we feel that 10 would be unlikely to have a ^{13}C signal at 154.0 ppm. Mechanisms can be drawn for the formation of RNCO^{2+} (on alkaline hydrolysis) from any of 7–10.

(ii) $\text{RN}(\text{CHO})_2^{2+}$. The deprotonated diformamide complex 11 was the major constituent of the second fraction to crystallize.



Its perchlorate salt is reasonably soluble in water, and the complex was recrystallized and characterized as the $\text{S}_2\text{O}_6^{2-}$ salt. Crystals of sufficient quality for X-ray structural analysis could not be grown. The ^1H spectrum (0.1 M DCl) gave a sharp 2-proton singlet at 8.73 ppm (vs ammine signals at 3.68 (12), 3.35 (3) ppm), and the ^{13}C spectrum a single absorption at 184.1 ppm. The IR spectrum showed a broad carbonyl absorption at 1603 cm^{-1} , which is to be compared with that for diformamide (1680 cm^{-1}) and its sodium salt (1575 cm^{-1}).²⁴ 11 moves as a 2+ ion on both HPIPC and ion-exchange chromatography, and N-coordinated amides are known to deprotonate readily.^{25,26} There seems little doubt

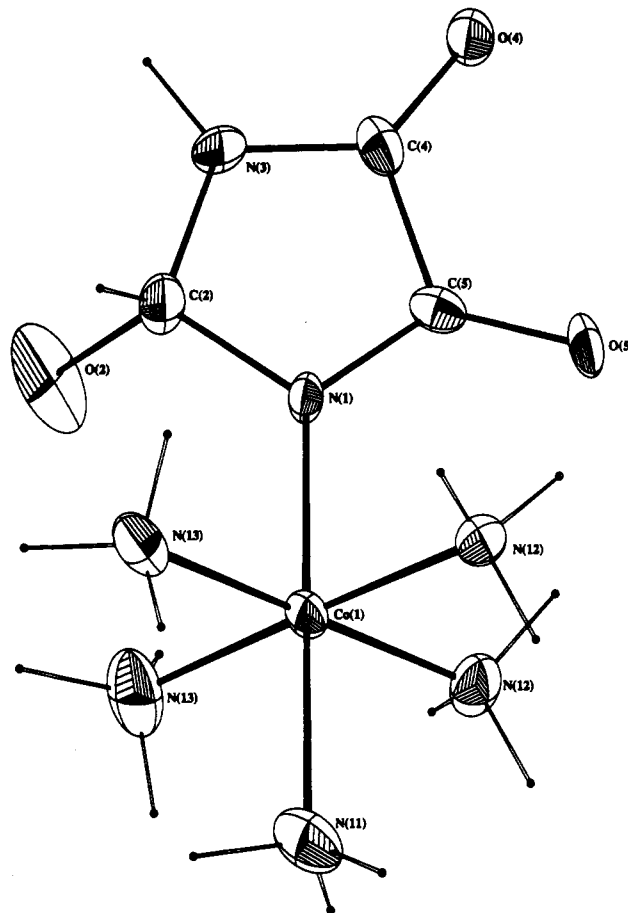


Figure 4. View of $\text{R}(2\text{-hydroxyimidazolidine-4,5-dione})^{2+}$ cation, 12, showing the atom-numbering scheme. Thermal ellipsoids enclose 50% probability levels.

Table V. Final Positional and Equivalent Thermal Parameters for $[(\text{NH}_3)_5\text{Co}(2\text{-hydroxyimidazolidine-4,5-dione})](\text{CF}_3\text{SO}_3)_2$

atom	x/a	y/b	z/c	$U_{\text{eq}}, \text{ \AA}^2$
Co(1)	0.6419 (1)	0.5000	0.4934 (2)	0.021
N(11)	0.6875 (4)	0.5000	0.315 (1)	0.036
N(12)	0.6704 (2)	0.672 (1)	0.6437 (9)	0.029
N(13)	0.6142 (2)	0.676 (1)	0.344 (1)	0.034
N(1)	0.5978 (3)	0.5000	0.668 (1)	0.025
C(2)	0.5541 (4)	0.5000	0.620 (2)	0.043
O(2)	0.5402 (5)	0.631 (4)	0.508 (2)	0.102
N(3)	0.5325 (3)	0.5000	0.794 (1)	0.026
C(4)	0.5585 (4)	0.5000	0.936 (2)	0.021
O(4)	0.5520 (2)	0.5000	1.100 (1)	0.028
C(5)	0.6023 (4)	0.5000	0.851 (2)	0.021
O(5)	0.6344 (3)	0.5000	0.950 (1)	0.025
S(1)	0.2867 (1)	0.0000	0.6999 (5)	0.030
O(11)	0.3293 (3)	0.0000	0.656 (2)	0.065
O(12)	0.2651 (3)	0.148 (2)	0.643 (2)	0.095
C(11)	0.279 (1)	0.0000	0.948 (3)	0.097
F(11)	0.2415 (5)	0.0000	0.981 (2)	0.171
F(12)	0.3025 (5)	0.118 (3)	1.019 (2)	0.225
S(2)	0.4085 (4)	0.0000	0.146 (2)	0.144
O(21)	0.4266 (4)	0.0000	0.296 (2)	0.044
O(22)	0.3906 (5)	0.137 (2)	0.040 (2)	0.118
C(21)	0.445 (2)	0.0000	-0.020 (6)	0.215
F(21)	0.456 (3)	0.0000	-0.34 (1)	0.511
F(22)	0.464 (1)	0.134 (4)	0.16 (2)	1.054

as to its identity as the N-bound diformamido complex. Despite much interest in diformamide in ab initio calculations,^{27–29} only two previous syntheses have been reported, both via derivatives

(22) Solomons, T. W. G. *Organic Chemistry*, 2nd ed.; Wiley: New York, 1980; p 666.

(23) Jackson, W. G. Personal communication.

(24) Allenstein, E.; Beyl, V. *Chem. Ber.* 1967, 100, 3551.

(25) Buckingham, D. A.; Clark, C. R. In *Comprehensive Coordination Chemistry*; Wilkinson, G., Gillard, R. D., McCleverty, J. A., Eds.; Pergamon: Oxford, England, 1987; Vol. 4, Chapter 47, p 682.

(26) Fairlie, D. P.; Jackson, W. G.; McLaughlin, G. M. *Inorg. Chem.* 1989, 28, 1983.

(27) Scuseria, G. E. *Chem. Phys.* 1986, 107, 417.

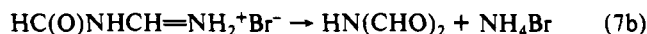
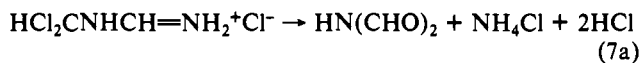
(28) Bock, C. W.; Trachtman, M.; George, P. *Chem. Phys.* 1981, 62, 303.

(29) Capparelli, A. L.; Maranon, J.; Sorarrain, O. M. *Z. Phys. Chem.* 1977, 258, 753.

Table VI. Selected Bond Lengths and Angles for [(NH₃)₅Co(2-hydroxyimidazolidine-4,5-dione)](CF₃SO₃)₂

Bond Lengths (Å)			
Co(1)-N(11)	1.99 (1)	C(2)-O(2)	1.39 (2)
Co(1)-N(12)	1.965 (8)	C(2)-N(3)	1.45 (2)
Co(1)-N(13)	1.971 (8)	N(3)-C(4)	1.30 (2)
Co(1)-N(1)	1.933 (9)	C(4)-O(4)	1.21 (1)
N(1)-C(2)	1.44 (1)	C(4)-C(5)	1.56 (2)
N(1)-C(5)	1.32 (1)	C(5)-O(5)	1.24 (1)
Bond Angles (deg)			
N(11)-Co(1)-N(12)	90.7 (3)	N(1)-C(2)-O(2)	115 (1)
N(11)-Co(1)-N(13)	88.9 (3)	N(1)-C(2)-N(3)	106.9 (9)
N(11)-Co(1)-N(1)	179.8 (2)	O(2)-C(2)-N(3)	110.1 (9)
N(12)-Co(1)-N(13)	89.5 (3)	C(2)-N(3)-C(4)	110.9 (9)
N(12)-Co(1)-N(1)	89.1 (3)	N(3)-C(4)-O(4)	129 (1)
N(13)-Co(1)-N(1)	91.3 (3)	N(3)-C(4)-C(5)	105.4 (9)
Co(1)-N(1)-C(2)	125.7 (7)	O(4)-C(4)-C(5)	125 (1)
Co(1)-N(1)-C(5)	126.0 (8)	N(1)-C(5)-C(4)	108.5 (9)
C(2)-N(1)-C(5)	108.3 (9)	N(1)-C(5)-O(5)	129 (1)
		C(4)-C(5)-O(5)	121.6 (9)

of formamidinium salts (eqs 7a and b).²⁴ The synthesis of **11** represents the first report of its formation as a ring degradation product of imidazole.



(iii) **R(2-hydroxyimidazolidine-4,5-dione)**²⁺. This complex, **12**, was the most soluble of the three complexes formed on treating RImH³⁺ with HOBr. It was isolated as its CF₃SO₃⁻ and Cl⁻ salts, and an X-ray structure was completed on the former.

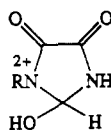
**12**

Figure 4 shows the complex cation and defines the atom-numbering scheme, and Tables V and VI give the crystallographic data. The poor data and disorder problems discussed in the Experimental Section preclude detailed discussion of the structural parameters, except that the bond lengths involving the carbonyl oxygens, C(4)-O(4) = 1.21 (1) Å and C(5)-O(5) = 1.24 (1) Å, and the hydroxyl group, C(2)-O(2) = 1.39 (2) Å, confirm the assignment of the complex as a 2-hydroxyimidazolidine-4,5-dione derivative. Carbonyl absorptions occurred at 1736 and 1664 cm⁻¹ in the IR spectrum; the ¹H NMR spectrum showed a single C-H proton at 5.78 ppm (H-2), and the ¹³C spectrum three absorptions due to the cation at 87.5, 162.4, and 172.3 ppm. The 87.5 ppm absorption confirms the presence of saturated carbon (C-2). The complex elutes as a 2+ ion on HPIPC, confirming deprotonation at coordinated nitrogen.

3. Comparisons with Earlier Studies. In the absence of buffers and at pH ~ 4 the reaction between Br₂(aq) and RImH³⁺ leads to the fully brominated imidazole complex **1** as the only product.¹ This species is reasonably acidic (pK_a ~ 1.83)² and exists as a 2+ ion in most aqueous solutions. It undergoes slow hydrolysis in acidic solution (H⁺-catalyzed) to give ROH₂³⁺ and 2,4,5-tribromoimidazole.² However, in the presence of buffers (AcO⁻, H₂PO₄⁻/HPO₄²⁻) the bromination of RImH³⁺ results in the fully oxidized product **2**, and this appears to result from AcOBr-catalyzed bromination of **1**, followed by hydrolysis. Neither **1** nor **2** is produced in significant amounts on treating RImH³⁺ with HOBr (in the presence of Ag⁺ ion), and ring degradation appears to be the most important reaction here. The mechanism of this reaction is not understood. However, one of the products, the hydroxy diketone **12**, does not produce **2** on treatment with Br₂(aq) in acetate buffer. Neither does **2** form **12** in the presence of HOBr. Thus, these two species must be formed by different reaction pathways.

Acknowledgment. We thank Dr. Ward T. Robinson, University of Canterbury, for the X-ray data collection.

Supplementary Material Available: Tables of thermal parameters of the non-hydrogen atoms, positional and thermal parameters for the calculated H atoms, mean plane data, and bond lengths and angles for **2** and **12** (7 pages); tables of observed and calculated structure factors for **2** and **12** (14 pages). Ordering information is given on any current masthead page.